Review paper: The 30th March 1986 M_w 5.7 Marryat Creek surface rupturing earthquake, Australia

Tamarah King

School of Earth Sciences, The University of Melbourne, Victoria 3010, Australia
tamarah.king@unimelb.edu.au
https://orcid.org/0000-0002-9654-2917

Mark Quigley

School of Earth Sciences, The University of Melbourne, Victoria 3010, Australia
Mark.quigley@unimelb.edu.au
https://orcid.org/0000-0002-4430-4212

Dan Clark

Geoscience Australia, Canberra 2601, Australia
https://orcid.org/0000-0001-5387-4404

Abstract

The 30th March 1986 M_w 5.7 Marryat Creek earthquake produced a highly arcuate 13 km long surface rupture with maximum vertical displacement of 0.9 m. Sinistral displacement on the NE-SW limb, dextral displacement on the NNE-SSW limb, and maximum vertical displacement in the central apex of rupture supports SW over NE movement of a hanging-wall block. Epicentre locations are poorly constrained and inaccurate, locally exceeding distances of 30 km from the surface rupture. The most geologically and seismologically reasonable fault rupture model involves 3 bedrock-controlled faults. Assuming simple planar geometry, these would intersect 5.5 km SW of the rupture at 3 km depth, which is consistent with centroid depths of 3 – 4.5 km. Two trenches across the 1986 rupture trace show no preceding discrete offset since deposition of overlying sediments (100 – 130 ka). Strong evidence exists to suggest historic surface rupture was controlled by basement structures including a large pre-existing fault, but only circumstantial evidence supports any prior neotectonic rupture. This earthquake is one of the most structurally complex (as proxied by the number of discrete faults) for its magnitude, as evidenced by comparison with a global compilation.

This document presents a review of available literature related to the 1986 Marryat Creek surface rupturing earthquake. It includes newly digitised data related to the rupture and new interpretations of controls on fault rupture. It supplements a manuscript reviewing all Australian surface rupturing earthquakes, submitted to Geosciences in August 2019.

Please contact authors on the content presented herein; we welcome constructive feedback.

---

1. Geology

1.1 Regional / background

The 1986 Marryat Creek, 2012 Pukatja and 2016 surface rupturing earthquakes occurred within the Musgrave Block, a Mesoproterozoic basement assemblage that extends across the Northern Territory / South Australia into Western Australia (Figure 1). This block is composed of high grade metamorphic and magmatic suites formed during the ~1200 Ma Musgrave orogen and reworked during the 580 - 520 Ma Petermann Orogeny (Aitken and Betts, 2009; Cawood and Korsch, 2008; Edgoose et al., 2004; Raimondo et al., 2010). Two large structures, the Woodroffe Thrust and Mann Fault, dominated uplift and deformation during the Petermann Orogeny (Lambeck and Burgess, 1992; Neumann, 2013; Stewart, 1995; Wex et al., 2019). The Woodroffe Thrust was responsible for significant exhumation of lower-crustal rocks, displacing the Moho by ~20 km associated with a present-day large gravitational and magnetic anomaly (Hand and Sandiford, 1999; Korsch et al., 1998; Wade et al., 2008). The Petermann and Pukatja surface ruptures occurred within 10 km of the Woodroffe Thrust (on the hanging-wall), and the Marryat Creek rupture is coincident with the location of the Mann Thrust as mapped by some authors (Aitken and Betts, 2009; Raimondo et al., 2010).
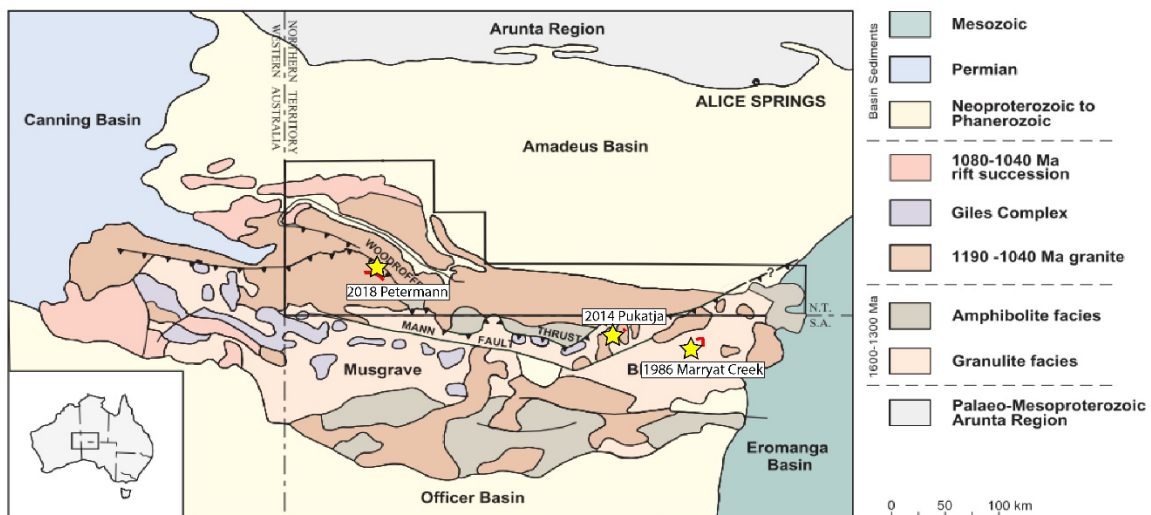
Figure 1: Musgrave Block geology from Figure 3 of Edgoose et al. (2004) with Petermann, Pukatja and Marryat Creek earthquakes (yellow stars) and ruptures (red lines) overlaid. Note some authors locate the Mann Fault further south than this map, coincident with the location of the Marryat Creek rupture (Aitken and Betts, 2009; Raimondo et al., 2010). *(CC) NT Gov*

1.2 Local bedrock

The Marryat Creek surface rupture occurred in an area where near-surface granitic metamorphic rocks are cross-cut by faults and dikes. The NE-SW limb of rupture (herein termed MC_1) is coincident with the location of the Mann fault as mapped by some authors (Aitken and Betts, 2009; Raimondo et al., 2010) visible as a linear magnetic anomaly striking east-west (Figure 3). Bedrock close to the surface rupture (0 - 5 km) occurs as low-lying isolated outcrops and is described as altered and deformed metamorphosed granite (Machette et al., 1993) (Figure 2, Figure 4). Dikes are mapped on the 1 : 250 000 geological map (Fairclough et al., 2011) and described by some authors investigating the historic surface rupture (Machette et al., 1993) within 5 km of the surface rupture in either a roughly NE-SW or NW-SE orientation (Figure 4). Bedrock outcrops visible on satellite imagery close to the surface rupture have three sets of structural / intrusive orientations matching the three main strike directions of the historic surface rupture (Figure 2, Figure 4). Small outcrops of gneissic bedrock are exposed in the hanging-wall adjacent to the Marryat Creek North trench site described in Machette et al. (1993).

67   The authors find that foot-wall bedrock is heavily sheared and altered in their trench (Section 4.2),
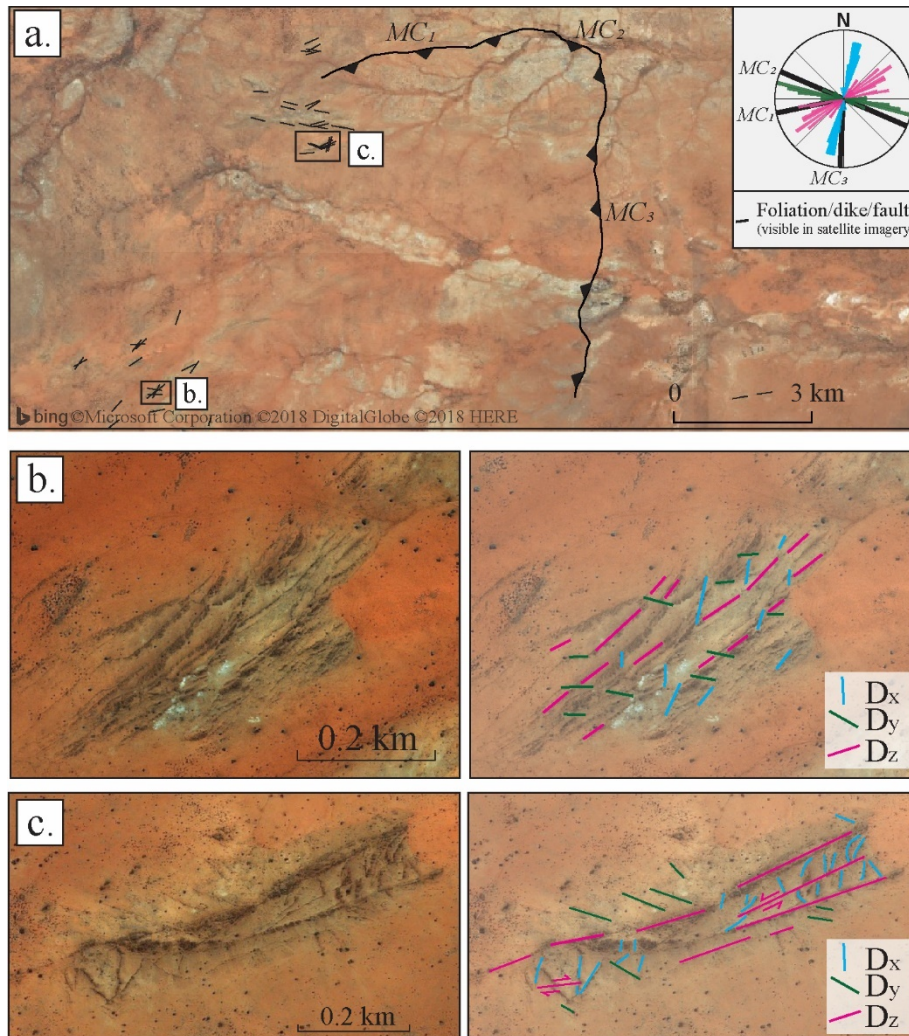68   which they attribute to a pre-existing fault.

69

Figure 2: Satellite imagery (Bing © 2019 DigitalGlobe, HERE, Microsoft) of outcrops close to the Marryat Creek rupture showing three clear sets of structural orientations

70   The MC$_1$ limb of the arcuate Marryat Creek scarp overlies and aligns with a linear magnetic anomaly
71   that displaces other north-south trending magnetic anomalies. This limb is also sub-parallel to a large
72   ~ 280 km long regional gravity anomaly (Figure 3). This anomaly is mapped by some authors as the
73   Mann Fault, a structure that extends across the Musgrave Block (Aitken and Betts, 2009; Raimondo et
74   al., 2010). The NNE-SSW limb of rupture (herein termed MC$_3$) is sub-parallel to pervasive NNE-
75   SSW fabrics apparent on the magnetic anomaly map. Multiple WNW-ESE linear anomalies are also
76   visible, aligning with the central section of the surface rupture (herein termed MC$_2$). The coincidence
77   between all three sections of surface rupture with bedrock orientations visible at the surface (Figure
78   2), and as pervasive linear magnetic anomalies (Figure 3) suggests that rupture was controlled by pre-
79   existing structures within the deformed and metamorphosed granitic basement (e.g. dikes, foliation,
80   faults). This is supported by trenching conducted across the rupture (see Section 10).
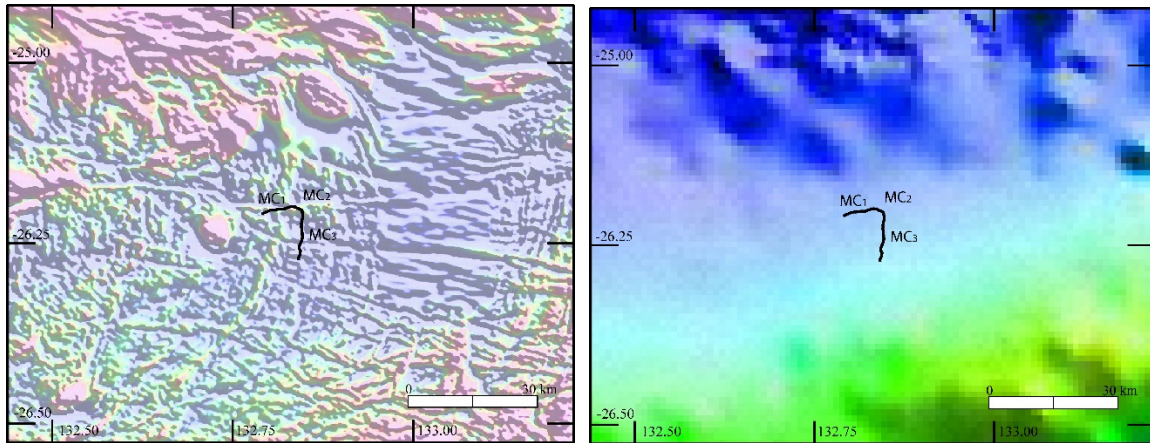
Figure 3: Marryat Creek scarp (black lines) relative to magnetic anomaly and bouguer gravity anomaly maps. National bouguer gravity anomaly map: http://pid.geoscience.gov.au/dataset/ga/101104. National total magnetic intensity map: http://pid.geoscience.gov.au/dataset/ga/89596

81   **1.3 Surficial deposits**

82   Bedrock is overlain by clastic alluvial, colluvial and aeolian sediments and soils (Figure 4) up to 10 m
83   thick in dunes and drainages , but generally < 3 m thick and underlain by gneissic or granulite
84   basement (as logged in water bore-hole data[1] surrounding the surface rupture at < 15 km distance).
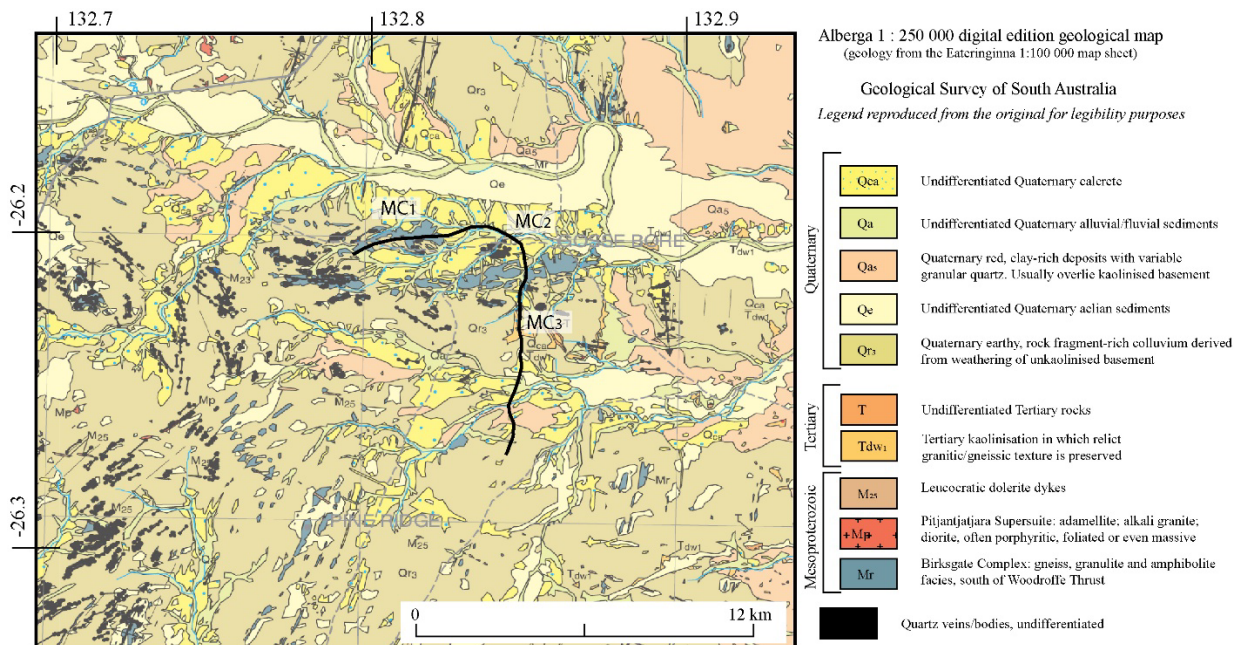
Figure 4: Crop of Alberga 1:250 000 digital edition geological map sheet (Fairclough et al., 2011) showing basement and surface sediments around the Marryat Creek surface rupture. Full map and legend available from Government of South Australia, Department for Energy and Mining: http://www.energymining.sa.gov.au/minerals/online_tools/free_data_delivery_and_publication_downl oads/digital_maps_and_data

85

---

[1] https://www.waterconnect.sa.gov.au/Systems/GD/Pages/Default.aspx

2. Seismology

2.1 Epicentre and magnitude

The Marryat Creek earthquake occurred more than 300 km from the nearest seismometer (Alice Springs). Some instrumental recordings were omitted from epicentral determinations due to high negative travel time residuals (between 5 – 17 degrees) (Barlow et al., 1986). The first published locations (Barlow et al., 1986) for the USGS place the epicentre ~ 15 km SW of the surface rupture, and for GA (then BMR) ~35 km SW of the rupture (this location is the current GA epicentre in the online catalogue). A revised location was published by McCue et al. (1987) ~ 5 km west of the surface rupture on the hanging-wall, but they do not elaborate on how this revision was made (it is assumed they located it relative to the surface rupture hanging-wall). Denham (1988) provide updated locations from the USGS, GA and one based on the surface rupture location. The recently published NSHA18 catalogue (Allen et al., 2018) places the epicentre ~ 15 km south-west of the rupture, it is unknown how this location was derived. The GA, USGS and NSHA18 epicentres do not lie close enough to the surface rupture location to be considered accurate. The only published uncertainty values are in the GA_online catalogue (± 1 km), and are considered lower that what is reasonable given the instrumental density (statistical uncertainties are considered to be closer to ± 10 km (Leonard, 2008)). The mis-location of seismological epicentres away from the surface rupture is a considered to be a combination of the velocity model used by each agency, and other epistemic uncertainties. These large epistemic uncertainties in epicentre location also affected foreshock and aftershock distributions (discussed below).

This paper prefers the magnitude (M_W 5.7) of the recently published NSHA18 catalogue (Allen et al., 2018) as they conduct a thorough and consistent reanalysis of Australian magnitude values, particularly to address inconsistencies in the determination of historic magnitude values. This is generally consistent with previously reported magnitude values (M_L/M_b/M_s 5.7 - 5.8).

Table 1 : Published epicentre locations, depths and magnitudes

| Reference	Agency	Latitude	± (km)	Longitude	± (km)	Depth (km)	± (km)	M1		M2	
GA_online	GA	-26.333	1	132.517	1	5		5.7	Mw	6	M_L
Barlow et al (1986)	GA	-26.33		132.52		0					
McCue et al (1987)	Rupture based	-26.22		132.82				5.7	Mb	5.8	Ms,
Allen et al (2018)		-26.31		132.734		5		5.7	Mw		
Barlow et al (1986)	Rupture based	-26.199		132.83							
Barlow et al (1986)	"South Australia"	-26.285		133.019		19		5.2	M_L		
Barlow et al (1986)	USGS	-26.23		132.7		10		5.8	Ms	5.7	Mb
Denham (1988)	Rupture based	-26.2		132.8				5.8	Ms		
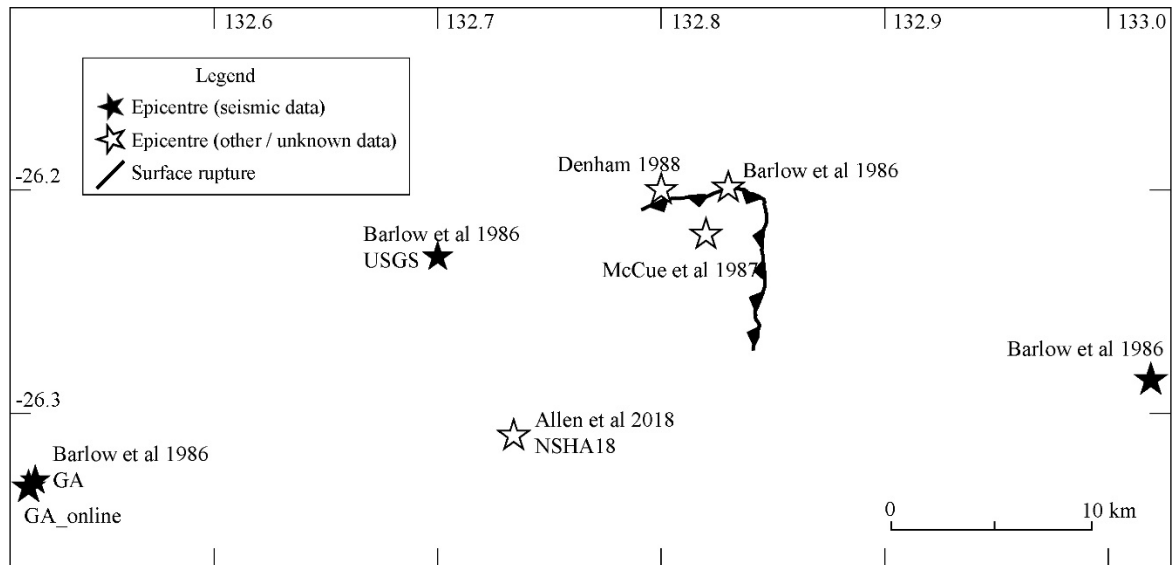
Figure 5: Published epicentre locations around the surface rupture.

2.2 Focal mechanisms

Three focal mechanisms are published for the Marryat Creek event; Barlow et al. (1986) (reproduced in (McCue et al., 1987)), Fredrich et al. (1988), and Global CMT (Ekström et al., 2012) (*Figure 6*). The Barlow et al. (1986) solution uses P-wave first motions and suggests a largely strike-slip component to movement, with the strike of either plane matching the trace of either limb of the surface rupture (which is highly arcuate). McCue et al. (1987) prefer the E-W plane of this solution which implies a sinistral movement on a steep 67° S dipping fault. Fredrich et al.(1988) invert teleseismic long- and short period P-waves, and long period SH-waves to derive their solution with an uncertainty of ± 20° on their focal mechanism strike. The arcuate surface rupture shows an overall west over east movement, and the west dipping CMT and Fredrich et al.(1988) solutions give a slightly dextral component of movement along a 35 - 42° SW dipping fault. A potential way to reconcile these focal mechanism solutions is a scenario where P-wave first motions represent an initial sub-event on a steep south or west dipping plane (e.g. MC_1 / MC_3), prior to the mainshock on a shallower SW dipping fault (e.g. MC_1) as recorded by teleseismic body-waves.
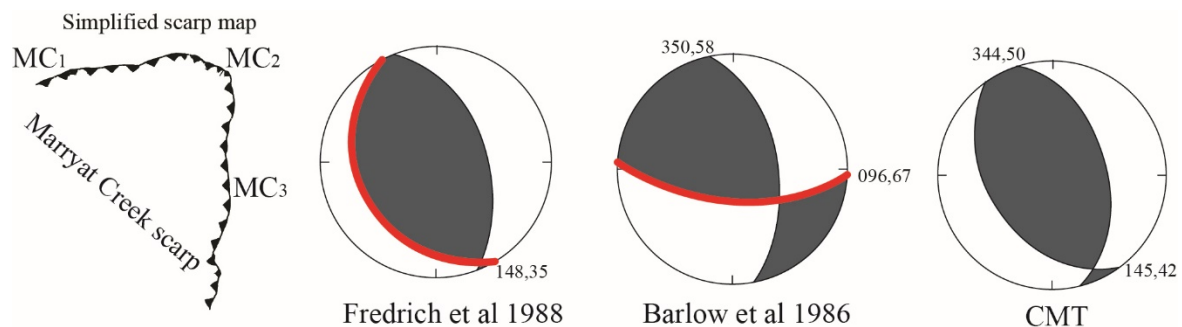
Figure 6: Published focal mechanism and simplified scarp map and preferred plane from the publication

2.3 Depth

Fredrich et al.(1988) find a centroid depth of 0 - 3 km based on inversion of long and short period waveforms. Boatwright and Choy (1992) analyse acceleration spectra from teleseismic data for the Marryat Creek event using a depth of 4.5 km, it is unclear what this depth is derived from. The GA_online catalogue and NSHA18 (Allen et al., 2018) report depths of 5 km but the justification for this depth is not stated. Barlow et al. (1986) report seismologically derived depths of 10 km and 19

133 km from different agencies, which are too deep to have caused a surface rupture for the moment of the
134 earthquake. Uncertainty bounds are not reported for any depth estimates.

135 ### 2.4 Foreshock / aftershocks

136 Large uncertainties due to poor instrumental density diminishes the ability to assess prior and post
137 mainshock seismic activity in the region. The GA database includes two M_L 3.0 events between 1900
138 and the 1986 mainshock. The first is 50 km SW of the rupture in August 1983, and the other 85 km
139 west in January 1985. Leonard (2008) suggests the national catalogue is complete for $M_L > 3.5$ from
140 1980, though the inclusion of these two events suggest the Marryat Creek area may have been
141 complete for > 3.0 by 1983. The events are likely to be poorly located, given the ~35 km distance
142 between the mainshock location and surface rupture. Many authors (Machette et al., 1993; McCue et
143 al., 1987; etc) state that the area was aseismic prior to the mainshock, but given the lack of
144 instrumentation available, the area may have experienced seismicity $M_L < 3.5$ prior to 1980 without
145 being detected.

146 Aftershock activity for the mainshock is likewise affected by poor instrumentation. Five aftershocks
147 M_L 3.0 - 3.3 were recorded in the seven days following the mainshock all poorly located (up to 100
148 km away from the rupture) with 13 other aftershocks recorded by the Alice Springs seismometer but
149 not located (McCue et al., 1987). McCue (1990) suggests that the Alice Springs seismometer was
150 capable of recorded seismic activity in the Marryat Creek area down to M_L 2.0. In July 1986 (4
151 months following the mainshock) a M_b 5.6 earthquake was recorded 8 km north of the GA epicentre
152 (Allen et al., 2018), and ~35 km west of the rupture. McCue (1990) reports a "a few small
153 aftershocks" from this event that aren't published or recorded, followed by a cessation of seismicity in
154 the region. A reconnaissance survey of the surface rupture was conducted prior to this event (Barlow
155 et al., 1986), constraining the surface rupture to the March event rather than a combination of the
156 March and July events which had similar magnitude values.

157 Eight temporary seismometers were deployed in 1990 (4 years after the mainshock) for 12 days with
158 two events detected (Machette et al., 1993). The authors regard the first, located 14 km NW, as
159 unrelated to the mainshock. The second, with a duration magnitude of 2 (Md) was located on the
160 hanging-wall ~1 km west of the scarp at a depth of 1.1 ± 1.4 km. If this earthquake occurred on the
161 seismogenic fault responsible for the MC_3 limb, it implies a fault dip of ~ 47°. No seismicity is
162 recorded in the GA online catalogue within 25 km of the rupture since 1986.

163 ## 3. Surface Rupture

164 ### 3.1 Authors / map quality

165 The Marryat Creek surface rupture is one of the least accessible of all historic Australian ruptures, a
166 370 km drive south of Alice Springs or 1300 km north from Adelaide. The rupture occurred within
167 the Anangu Pitjantjatjara Yankunytjatjara (APY) area of South Australia, making access dependant on
168 permits. Despite the remoteness, detailed surveying was conducted along the length of rupture to
169 characterise offset (Bowman and Barlow, 1991), aerial photography was obtained to help map the
170 rupture, and multiple trenches were dug to characterise geometry and palaeoseismicity (Machette et
171 al., 1993). The few published aerial images of the scarp (e.g. figure 8 Machette et al. (1993)) and
172 1:500 maps (Plate 2 (Machette et al., 1993)) show rupture complexity with duplexing ruptures,
173 hanging-wall folding / cracking, and small < 20 m steps in rupture. This complexity is not captured in
174 the published 1 : 10 000 and 1 : 50 000 maps of the rupture (e.g. (Bowman and Barlow, 1991;
175 Machette et al., 1993)). The rupture trace from the GA Neotectonics Features database (Clark et al.,
176 2012) and sections visible in Google and Bing satellite imagery do not align, due to datum
177 transformation issues and simplification of fine-scale morphology in the original map.

178 ### 3.2 Length and shape

179 The Marryat Creek scarp is highly arcuate in a concave direction (relative to the hanging-wall) with
180 an 8 km distance between end points. The trace length of published maps of the rupture (Figure 7a) is
181 between 13.8 -14.2 km (Bowman and Barlow, 1991; Machette et al., 1993). Bowman and Barlow
182 (1991) describe lengths of 5.5 km for MC_1 and 7.5 km for the MC_3 (13 km total) where the mid-
183 section of rupture (MC_2) is captured in the length of MC_1 (Figure 7b). A length of 13 km is used
184 across publications describing the rupture (Barlow et al., 1986; Machette et al., 1993; McCue, 1990;
185 McCue et al., 1987). Applying a criteria which simplifies ruptures to straight traces and defines
186 distinct faults where mapped primary rupture has gaps/steps > 1 km and/or where strike changes by >
187 20° for distances > 1 km (e.g. (Quigley et al., 2017)) results in three faults with a total length of 13.6
188 km (Figure 7c) (explored in more detail in King et al. (2019) (in review)).

189 Figure 7d presents portions of the scarp where more than two vertical displacement measurements of
190 greater than 0.2 m occur within a distance of 1 km (data from Bowman and Barlow (1991)). Applying
191 cosmogenic erosion rates from lithologically and climatically analogous settings of Australia (0.3 – 5
192 m/Myr; Bierman and Caffee, 2002) suggests that 0.2 m of scarp height could be removed within 35 –
193 660 kyrs, leaving just 1 km of rupture length (i.e., 1 km of residual surface rupture with relief ≥ 0.2m)
194 visible in the landscape. This suggests that the surface scarp may not persist within this landscape as a
195 mappable scarp, unless recurrence intervals are < 0.5 to 1 Myr. Potential recurrence on this fault is
196 limited by trenching results (Section 4) to > 130 ka (Machette et al., 1993). In this calculation we
197 assume that the scarp is shallowly underlain by granitic bedrock and that the scarp erodes more
198 rapidly than the surrounding terrain at rates commensurate with Bierman and Caffee (2002). We do
199 not account for erosion rates of any duricrust which may overlie granitic bedrock or
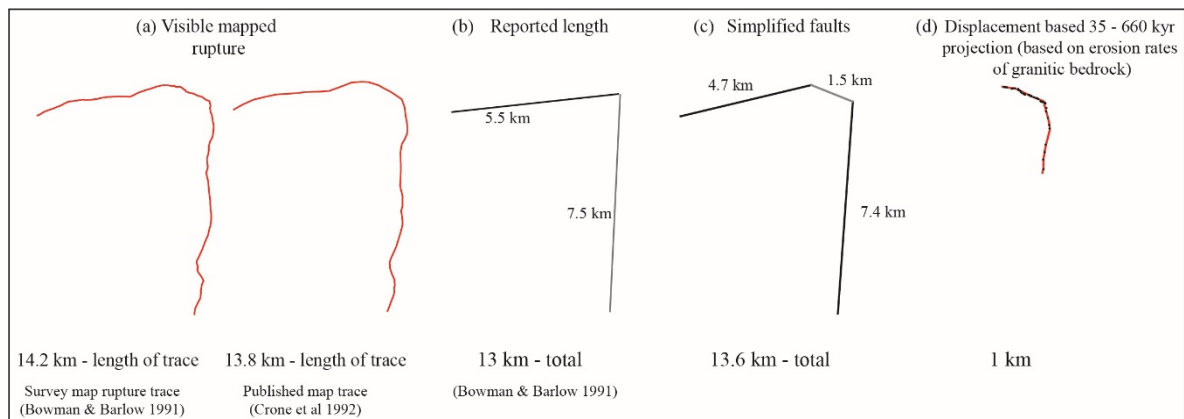200 anthropogenically- and/or climatically-modulated variations in erosion rates.

Figure 7: *Measures of length for the Marryat Creek surface rupture and underlying faults.*

3.3 Strike

202 The strike of the Marryat Creek rupture is highly variable due to the arcuate nature, with MC_1
203 trending 078°, MC_2 trending 117° and MC_3 trending 184° (Bowman and Barlow, 1991; Machette et
204 al., 1993). A line drawn between end points trends 145°. The three main directions of surface rupture
205 strike are shown relative to basement structural trends in *Figure 2*.

3.4 Dip

207 Cross sections across the rupture are shown in detailed survey maps presented in Bowman and Barlow
208 (1991) including three with dip measurements (Figure 8). It is unclear if these measurements are from
209 small trenches dug by the surveyor, from natural exposures of the rupture plane, or from calculations
210 of dip based on vertical offset and heave. Machette et al. (1993) present two measurements of dip
211 from trenches dug across the rupture (Figure 8). Together these dip measurements range from 36 –
212 60°, averaging 51° along MC_2 and MC_3. No dip measurements are recorded from MC_1.

213   Fredrich et al. (1988) prefer a dip of 35° ± 20 on a SW dipping plane from teleseismic body wave
214   inversion while Barlow et al. (1986) prefer a dip of 67° on a south dipping plane based on p-wave first
215   motions. These dips may be representative of an initial sub-event on MC_1 or MC_3 as described by P-
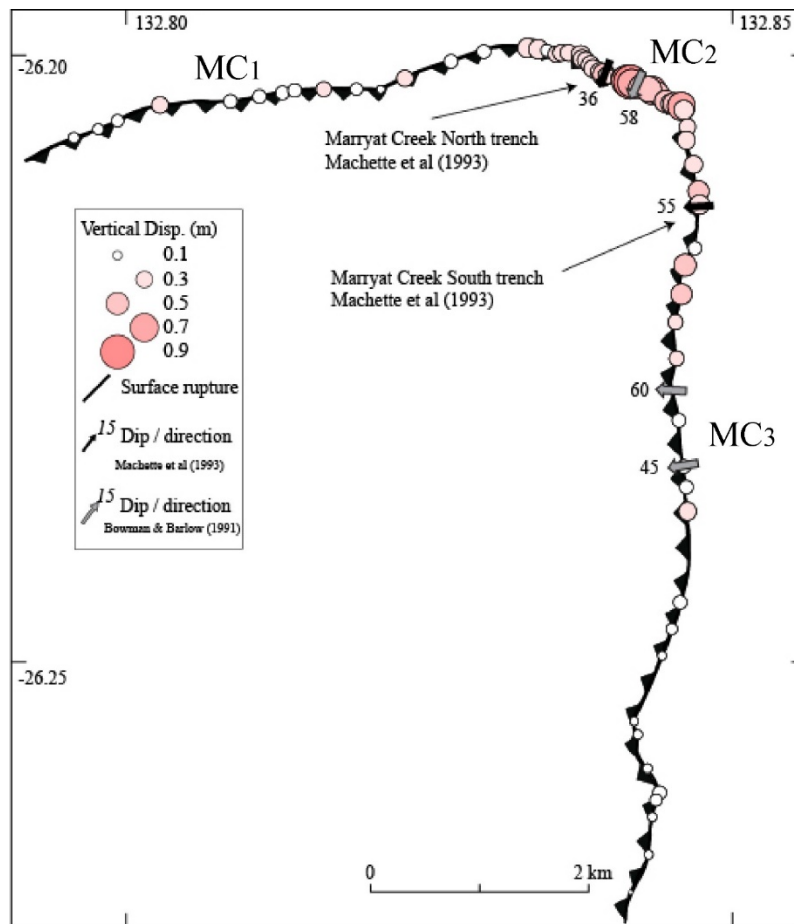216   wave first motions, followed by a mainshock on MC_2 as described by body-waves.

Figure 8 Map of the Marryat Creek scarp, vertical offset measurements, dip measurements and trench sites (digitised from Bowman and Barlow (1991) and Machette et al. (1993)).

217   ### 3.5 Morphology

218   Machette et al. (1993) conducted their field mapping four years after the earthquake with much of the
219   rupture and surface features still visible, though smaller details were destroyed by erosion and cattle.
220   They describe the rupture as discrete with minor hanging-wall folding, or expressed as warping of the
221   ground surface into a pressure ridge. The authors note en-echelon steps in the scarp separated by
222   ramps or monoclines, though they do not mention the lengths, widths or directions of these features.
223   An aerial photograph in McCue et al. (1987) shows ~10 - 20 m long duplexing discrete ruptures with
224   an en-echelon, back-stepping morphology.

225   ### 3.6 Lateral displacement

226   Barlow et al. (1986) published the first description of the surface rupture and note left-lateral slip on
227   MC_1 and right-lateral slip on MC_3. Figure 3 of McCue et al. (1987) shows right-stepping transpression
228   in discrete rupture on MC_3. Offsets of pre-existing animal and vehicle tracks were measured to
229   estimate sinistral lateral offsets of 0.8 m on MC_1 (McCue et al., 1987) though these data are not
230   presented in a map. A tree trunk was observed overlying part of MC_1, with a clear pre-event trunk
231   impression on the ground showing 50 cm sinistral offset of the hanging-wall relative to foot-wall

232 (sheet 10, (Bowman and Barlow, 1991)). No measurable lateral offsets are recorded for the MC_3 in
233 any vehicle tracks or creeks that cross the scarp (Bowman and Barlow, 1991).

3.7 Displacement

235 Surveying along the rupture was conducted by the Australian Surveying and Land Information Group
236 (now merged into Geoscience Australia) in April and August 1986. No uncertainties are specified for
237 the surveying or levelling data, though Bowman and Barlow (1991) note that some error exists in
238 vertical displacement measurements due to difficulties estimating scarp height in sandy terrain. Ten
239 detailed profiles were collected, along dry creek beds where possible. Vertical displacement
240 measurements and profiles shows that vertical displacement reaches a maximums of 0.5 - 0.9 m
241 across 700 m along MC_2 and diminishes to < 0.25 m for the last 4 km of each limb.

242 Machette et al. (1993) appear to incorrectly reproduce some of the Bowman and Barlow (1991)
243 displacement data due to conversion errors. This data is replicated in scaling relationships of
244 Wesnousky (2008) and subsequent publications. We recommend referring to the data tables in
245 Bowman and Barlow (1991), or King et al. (2019) (in review).

246 Due to the remote nature, no absolute offset measurements are available from resurveyed benchmarks,
247 and no data regarding distributed deformation exist in the literature.
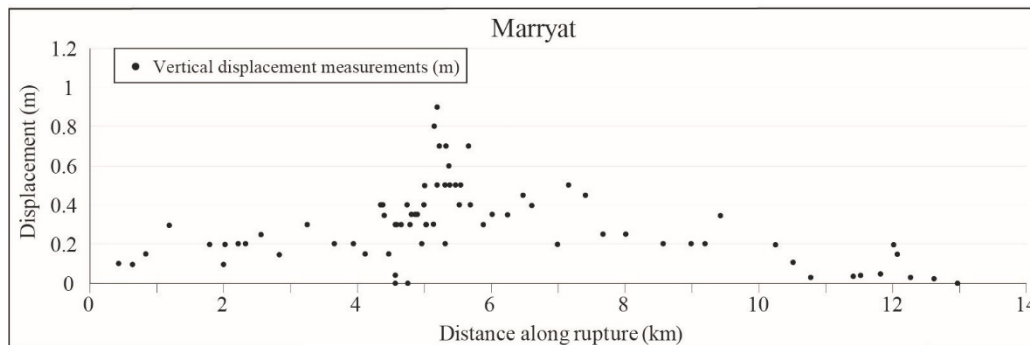

Figure 9 Vertical displacement measurements along the Marryat Creek scarp, digitised from Bowman and Barlow (1991). Methods described in Appendix A.

3.8 Environmental damage

249 Offset and length of the Marryat Creek surface rupture matches ESI IX – X (Michetti et al., 2007).
250 Minimal fracturing is described in field studies of this earthquake, and none is shown on the maps.
251 From descriptions and published images of the rupture, fracture lengths and widths are assigned ESI
252 VII within a few meters of the surface rupture. Multiple authors describe grass and bushes killed from
253 root tear on the hanging-wall at distances of 5 m (Bowman and Barlow, 1991; McCue et al., 1987).
254 Rabbit warrens on the hanging-wall within ~10 m were observed to have collapsed, though warrens at
255 similar distances on the foot-wall were intact (McCue et al., 1987). This vegetation and surface
256 damage does not fall within the scope of the ESI-07 scale (Michetti et al., 2007). No authors report
257 investigating bedrock outcrops in the area, so it is unknown whether rockfalls occurred or not.
258 Similarly, no publications discuss hydrological anomalies in any nearby bores.

4. Paleoseismology

4.1 Summary

261 Machette et al. (1993) present detailed analysis of two trenches and eight samples taken for grain size
262 analysis, uranium trend analysis and thermoluminescence dating. This work is also described in Crone
263 et al. (1997).

264 **4.2 Trenching**

265 **4.2.1. Identified units**
266 Machette et al. (1993) includes comprehensive descriptions of units identified in two trenches
267 (Marryat Creek South across MC_3 and Marryat Creek West across MC_2, *Figure 8*) and present a
268 summary of exposed units alongside interpreted trench logs in Plate 1 of that report. The trenches are
269 located on either side of the apex of rupture, in the area of maximum vertical offset. The western
270 trench is ~10 m north of a dry creek bed, and the trench cuts across a small, low outcrop of "sheared
271 granite" (granitic gneiss) on the hanging-wall. The southern trench is located just north of a very small
272 dry tributary that eventually feeds into the Marryat Creek. Both trenches were 2 - 2.5 m deep with
273 exposed bedrock at 0.3 and 1.25 m (west and south respectively). The authors interpret both trenches
274 to show evidence of "ancient" (presumedly 580 - 520 Ma Petermann Orogeny) faulting, but no
275 evidence of prior Cenozoic movement.

276 Bedrock in the MC_2 trench is described as 'fractured', 'sheared' and 'altered' granite. The fractured
277 granite is described as having recognisable fabric and mineralogy, the sheared portions retain only
278 some original granitic fabric and mineralogy, and the 'altered' granite is described as "extensively
279 altered and sheared into light-greenish-gray clay". The altered granite is more abundant on the foot-
280 wall, while the fresher granite is all on the hanging-wall.

281 Bedrock in the MC_3 trench is assumed to be originally basaltic and described as "altered rock
282 (greenstone)", "sheared rock (greenstone)" and "fractured rock (greenstone)" with the same
283 designation of 'fractured', 'altered' and 'sheared' as in the MC_2 trench granites. Unlike the MC_2
284 trench, the majority of 'fractured' greenstone (i.e. freshest) is found on the foot-wall of the modern
285 rupture. The authors suggest that the extreme brecciation of the foot-wall bedrock in both trenches
286 provides evidence of ancient faulting with "significant amount of differential movement" considering
287 the width and extent of foot-wall alteration (>10's of meters). They identify that while some blocks of
288 fresher granite are gradational into altered granite, some blocks with significantly different alteration
289 levels are juxtaposed together along planes with the same geometry as the 1986 rupture.

290 Surficial sediments in the MC_2 trench are 15 - 30 cm thick and include 10 - 20 cm of eolian sand and
291 14 - 30 cm of poorly sorted fluvial gravel with 2 - 3 cm subangular to subrounded gravel clasts
292 (Machette et al., 1993). The authors describe a weakly formed soil profile through the eolian sand and
293 fluvial gravel and suggest that the soil profile is less developed on the hanging-wall of the rupture.
294 Surficial sediments in the MC_3 trench are 0.7 - 1.2 m thick and include 10 - 20 cm of eolian sand, 0.05
295 - 0.75 m of poorly sorted sandy colluvial and fluvial gravel consisting of 1 - 2 cm clasts (up to 20 cm),
296 and 0.75 - 1.25 m of poorly sorted gravel with clasts reflecting local bedrock. The authors identify a
297 soil profile in the gravels that predates deposition of the eolian sands, but efforts to date the sediments
298 using uranium trend analysis were unsuccessful, and no suitable material was found for radiocarbon
299 dating. The authors instead use clay content, stratification and formation rates of calcium carbonate in
300 the soil to estimate a 52 - 130 ka oldest depositional age for the quaternary sediments identified, with
301 a preference for the older estimate.

302 **4.2.2. Structural interpretations**
303 In the MC_2 trench Machette et al. (1993) interpret basement geology to show that displacement in the
304 1986 earthquake was accommodated on a single fault plane that aligns to a pre-existing ancient fault.
305 Extensional fractures on the hanging-wall are identified within 1.25 m of the rupture related to
306 collapse of the hanging-wall block. The authors measure 46 - 47 cm of displacement across the base
307 of surficial sediments, with additional offset from minor hanging-wall folding.

308 A similar set of structures are observed in the MC_3 trench, with displacement confined to a single 25 -
309 30 cm wide fault zone with the same orientation as gouge and calcium carbonate veins found in the
310 heavily altered greenstone basement. No cracking or jointing is identified in this trench.

311 Displacements identified in the trenches match those measured at the surface, showing only historic
312 offset of sediments overlying a bedrock fault structure presumably related to the Petermann orogeny
313 (see Section 1.1).

4.3 Topography

315 McCue et al. (1987) note that the N-S rupture limb follows a linear topographic 'mound' for a few
316 kilometres and suggest this may provide geomorphic evidence for a prior relief-generating event.
317 However, Machette et al. (1993) consider the ridge to delineate differential erosion across resistant
318 bedrock as it is not a persistent feature along the rupture, and their trench observations show no
319 evidence of prior offset. Crone et al. (1997) suggest that the linear topographic high combined with a
320 greater number of low sporadic bedrock outcrops on the hanging-wall compared to the foot-wall
321 provide circumstantial evidence for prior Quaternary rupture. The distribution of bedrock on the
322 hanging-wall compared to the foot-wall is consistent with differential erosion of bedrock affected by
323 substantial Proterozoic fault movement and is not considered diagnostic of Quaternary rupture.

4.4 Slip rate

325 The strongest evidence for prior rupture comes from distinct boundaries between some semi-coherent
326 basement blocks and heavily altered basement in trenches described by Machette et al. (1993). These
327 semi-coherent blocks may have been faulted against altered material by prior Quaternary ruptures,
328 though this evidence is circumstantial and may also relate to older faulting. Overall, there is no strong
329 evidence to show any prior Quaternary rupture along the faults that hosted the 1986 Marryat Creek
330 earthquake, and trenching shows an absence of rupture since 130 ka (the preferred depositional age
331 described in Machette et al. (1993)).

332 The rupture is either the first Neotectonic event, or the recurrence interval is sufficiently long that all
333 relief relating to prior event(s) was eroded prior to 130 ka. If recurrence is assumed, vertical relief
334 generation rates are limited by very low bedrock erosion rates of < 5 m/Myr (Belton et al., 2004;
335 Bierman and Caffee, 2002).

5. Summary

5.1 Surface rupture relationship to Geology

338 Machette et al. (1993) find evidence that at least across MC_2 and MC_3, rupture propagated along a
339 fault presumably related to Neoproterozoic orogeny of the Musgrave Block. This is consistent with
340 geophysical data which shows linear magnetic anomalies in this location with orientations colinear to
341 both MC_2 and MC_3. The magnetic anomaly co-located with MC_1 is considered by some authors as the
342 location of the Mann Fault (Aitken and Betts, 2009; Raimondo et al., 2010), a major Neoproterozoic
343 crustal structure.

344 Large outcrops of gneiss within 1.5 km of the end of MC_1 and 4 km of MC_3 show three sets of dike,
345 fault and foliation orientations (*Figure 2*). These outcrops are not shown on the Machette et al. (1993)
346 geological map but are mapped on the 1 : 250,000 geological map of the area (Fairclough et al., 2011)
347 and are visible in satellite imagery (*Figure 2*).

348 A NW-SE trending linear magnetic anomaly ~ 5.5 km SW of the surface rupture is coincident with
349 the orientation of MC_2. This feature crosses MC_3 coincident with a distinct bend in the rupture trace.
350 The trend of this feature is within 025° of the strike of both preferred focal mechanism planes (which
351 have uncertainties of ± 020°) (Barlow et al., 1986; Fredrich et al., 1988). While there are no
352 constraints on the depth, dip or dip direction of this linear magnetic anomaly, we hypothesise that it
353 may represent the seismogenic fault as it's strike and location are coincident with seismogenic data
354 and fault geometry.

5.2 Surface rupture relationship to Seismology

356 Sinistral displacement on MC_1, dextral displacement on MC_3, and maximum vertical displacement on
357 MC_2 support SW over NE movement of a hanging-wall block, consistent with two of the three
358 published focal mechanisms. Trenching suggests that MC_2 is a through-going fault plane rather than
359 potentially representing a near-surface linkage structure between MC_1 and MC_3 (e.g. as hypothesized
360 for the 1968 Meckering surface rupture in Dentith et al. (2009)).

361 Due to poor instrumental coverage, epicentral locations and depths are highly uncertain and do not
362 help to constrain rupture dynamics or fault geometry. A highly simplified cross section (*Figure 10*)
363 across MC_1 and MC_3 using dip estimates based on surface measurements (corrected for apparent dip)
364 and assuming two fault planes extend to depth, shows a conjugate intersection of structures at ~ 1.8
365 km depth. This fault intersection reaches 3 km depth (centroid depth derived by Fredrich et al. (1988))
366 approximately 5.5 km south west of the central section of rupture, coincident with the NE-SW
367 trending magnetic anomaly described above.

368 Our preferred hypothesis to describe available seismological data (centroid depth and focal
369 mechanisms), geophysical data (three sets of linear magnetic anomalies coincident with surface
370 rupture orientations) and surface rupture measurements (maximum slip associated with the central
371 section of ruptures, measured dips, and lateral kinematics) is: rupture initiating on a fault related to
372 either MC_1 or MC_3 (or the intersection thereof) as described in P-wave first motion data (Barlow et
373 al., 1986); rupture propagating onto a NW-SE orientated, SW dipping fault (e.g. MC_2) consistent with
374 focal mechanisms from CMT and teleseismic body-waves (Ekström et al., 2012; Fredrich et al.,
375 1988); a centroid of slip release at ~ 3 km depth ~ 5.5 km SW of MC_2 coincident with the intersection
376 of the three prevailing planar bedrock structures; rupture propagating upwards along the SW dipping
377 fault towards the surface rupture location of MC_2, and bilaterally across MC_1 and MC_3 resulting in
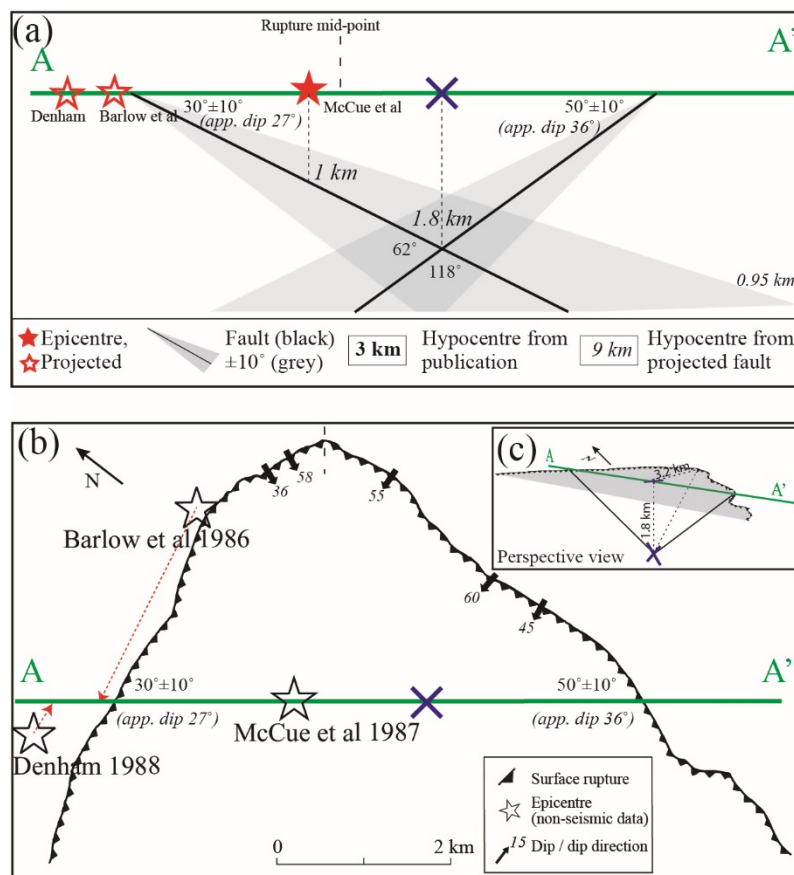378 lateral offsets along the limbs and maximum slip in the central area.

Figure 10: Highly simplified cross section of the Marryat Creek scarp as two faults, using surface
measurements of dips (± 10°, corrected to apparent dip), with published epicentres projected onto

the cross section showing depth to simplified faults (italics), and published depths (bold). (c) shows
a perspective view of the cross section (a) and map (b).

379

380 The number of distinct faults that are hypothesized to have ruptured in this earthquake (n=3), based on
381 the criteria stated herein, is the highest estimate of multi-fault earthquakes at this magnitude (M_w 5.7)
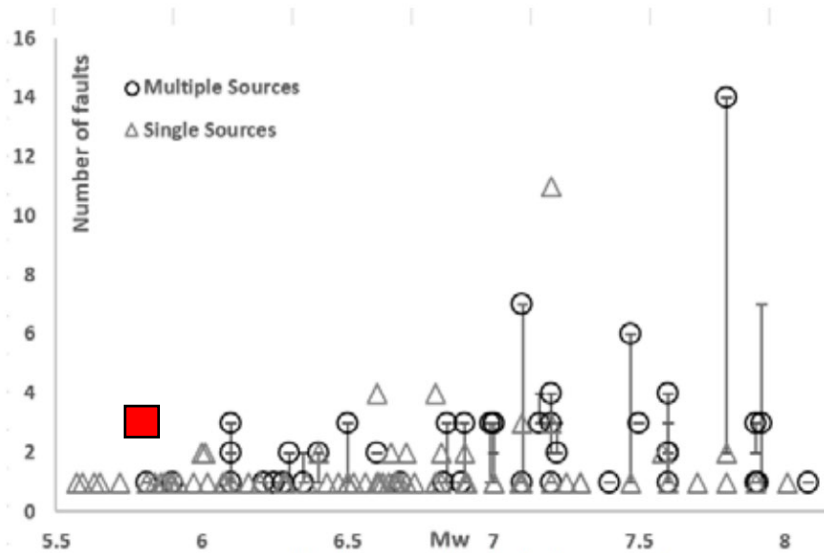382 as ascertained from a recent global compilation (Figure 11).

Figure 11 :From Fig. 5 of Quigley et al. (2017), Marryat Creek earthquake (red box) plotted
against recent global compilation of number of geometrically-distinguished fault ruptures vs.
Mw.

383

384

392

6. References

394 Aitken, A., Betts, P.G., 2009. Constraints on the Proterozoic supercontinent cycle from the structural
395   evolution of the south-central Musgrave Province, central Australia. Precambrian Res. 168, 284–
396   300. https://doi.org/10.1016/j.precamres.2008.10.006

397 Allen, T., Leonard, M., Ghasemi, H., Gibson, G., 2018. The 2018 National Seismic Hazard
398   Assesment: Earthquake epicentre catalogue (GA Record 2018/30). Geoscience Australia,
399   Commonwealth of Australia, Canberra, ACT.
400   https://doi.org/http://dx.doi.org/10.11636/Record.2018.030

401 Barlow, B.C., Denham, D., Jones, T., McCue, K., 1986. The Musgrave Ranges earthquake of March
402   30, 1986. Trans. R. Soc. South Aust. 110, 187–189.
403   https://doi.org/10.1126/science.97.2526.482-a

404 Belton, D.X., Brown, R.W., Kohn, B.P., Fink, D., Farley, K.A., 2004. Quantitative resolution of the
405   debate over antiquity of the central Australian landscape: Implications for the tectonic and
406   geomorphic stability of cratonic interiors. Earth Planet. Sci. Lett. 219, 21–34.
407   https://doi.org/10.1016/S0012-821X(03)00705-2

408 Bierman, P.R., Caffee, M.W., 2002. Cosmogenic exposure and erosion history of Australian bedrock
409   landforms. Bull. Geol. Soc. Am. 114, 787–803. https://doi.org/10.1130/0016-
410   7606(2002)114<0787:CEAEHO>2.0.CO;2

411 Boatwright, J., Choy, G.L., 1992. Acceleration source spectra anticipated for large earthquakes in
412   northeastern North America. Bull. Seismol. Soc. Am. 82, 660–682.

413 Bowman, J.R., Barlow, B.C., 1991. Surveys of the Fault Scarp of the 1986 Marryat Creek, South
414   Australia, Earthquake (BMR Record 1991/109). Australian Seismological Centre, Bureau of
415   Mineral Resources, Canberra, ACT.
416   https://doi.org/http://pid.geoscience.gov.au/dataset/ga/14490

417 Cawood, P.A., Korsch, R.J., 2008. Assembling Australia: Proterozoic building of a continent.
418   Precambrian Res. 166, 1–35. https://doi.org/10.1016/j.precamres.2008.08.006

419 Clark, D., McPherson, A., Van Dissen, R.J., 2012. Long-term behaviour of Australian stable
420   continental region (SCR) faults. Tectonophysics 566–567, 1–30.
421   https://doi.org/10.1016/j.tecto.2012.07.004

422 Crone, A.J., Machette, M.N., Bowman, J.R., 1997. Episodic nature of earthquake activity in stable
423   continental regions revealed by palaeoseismicity studies of Australian and North American
424   quaternary faults. Aust. J. Earth Sci. 44, 203–214. https://doi.org/10.1080/08120099708728304

425 Denham, D., 1988. Australian seismicity - the puzzle of the not-so-stable continent. Seismol. Res.
426   Lett. 59, 235–240. https://doi.org/https://doi.org/10.1785/gssrl.59.4.235

427 Dentith, M., Clark, D., Featherstone, W.E., 2009. Aeromagnetic mapping of Precambrian geological
428   structures that controlled the 1968 Meckering earthquake (Ms 6.8): Implications for intraplate
429   seismicity in Western Australia. Tectonophysics 475, 544–553.
430   https://doi.org/10.1016/j.tecto.2009.07.001

431 Edgoose, C.J., Scrimgeour, I.R., Close, D.F., 2004. Geology of the Musgrave Block, Northern
432   Territory (NTGS Report 15). Northern Territory Geological Survey, Darwin, Australia.

433 Ekström, G., Nettles, M., Dziewoński, A.M., 2012. The global CMT project 2004-2010: Centroid-
434   moment tensors for 13,017 earthquakes. Phys. Earth Planet. Inter. 200–201, 1–9.
435   https://doi.org/10.1016/j.pepi.2012.04.002

436 Fairclough, M.C., Sprigg, R.C., Wilson, B., Coats, R.P., 2011. Alberga 1:250 000 Geological Map,
437   Digital Edition. Geological Survey of South Australia, Adelaide, Australia.

438 Fredrich, J., Mccaffrey, R., Denham, D., 1988. Source parameters of seven large Australian
439   earthquakes determined by body waveform inversion. Geophys. J. 95, 1–13.
440   https://doi.org/https://doi.org/10.1111/j.1365-246X.1988.tb00446.x

441 Hand, M., Sandiford, M., 1999. Intraplate deformation in central Australia, the link between
442   subsidence and fault reactivation. Tectonophysics 305, 121–140. https://doi.org/10.1016/S0040-
443   1951(99)00009-8

444 King, T.R., Quigley, M.C., Clark, D., 2019. Surface-rupturing historical earthquakes in Australia and
445   their environmental effects: new insights from re-analyses of observational data. Geosciences.

446 Korsch, R.J., Goleby, B.R., Leven, J.H., Drummond, B.J., 1998. Crustal architecture of central
447   Australia based on deep seismic reflection profiling. Tectonophysics 288, 57–69.
448   https://doi.org/10.1016/S0040-1951(97)00283-7

449 Lambeck, K., Burgess, G., 1992. Deep crustal structure of the musgrave block, central australia:
450   Results from teleseismic travel-time anomalies. Aust. J. Earth Sci. 39, 1–19.
451   https://doi.org/10.1080/08120099208727996

452 Leonard, M., 2008. One hundred years of earthquake recording in Australia. Bull. Seismol. Soc. Am.
453   98, 1458–1470. https://doi.org/10.1785/0120050193

454 Machette, M.. M.N., Crone, A.. A.J., Bowman, J.R., Bowman, R.J., Bowman, J.R., 1993. Geologic
455   investigations of the 1986 Marryat Creek, Australia, earthquake: implications for
456   paleoseismicity in stable continental regions (USGS Bulletin 2032-B). Washington, USA.
457   https://doi.org/https://doi.org/10.3133/b2032B

458 McCue, K., 1990. Australia's large earthquakes and Recent fault scarps. J. Struct. Geol. 12, 761–766.
459   https://doi.org/10.1016/0191-8141(90)90087-F

460 McCue, K., Jones, T., Michael-Leiba, M., Barlow, B.C., Denham, D., Gibson, G., 1987. Another chip
461   off the old Australian block. Eos, Trans. Am. Geophys. Union 68, 609.
462   https://doi.org/10.1029/eo068i026p00609

463 Michetti, A.M., Esposito, E., Guerrieri, L., Porfido, S., Serva, L., Tatevossian, R.E., Vittori, E.,
464   Audemard M., F.A., Azuma, T., Clague, J., Comerci, V., Gurpinar, A., McCalpin, J.P.,
465   Mohammadioun, B., Morner, N.A., Ota, Y., Roghozhin, E., 2007. Intensity Scale ESI 2007,
466   Memorie Descrittive della Carta Geologica d'Italia, Special Volume 74. APAT, Rome 2007.

467 Neumann, N.L., 2013. Yilgarn Craton – Officer Basin – Musgrave Province Seismic and MT
468   Workshop (GA Record 2013/28). Geoscience Australia, Commonwealth of Australia, Canberra,
469   ACT. https://doi.org/http://pid.geoscience.gov.au/dataset/ga/76664

470 Quigley, M.C., Mohammadi, H., Duffy, B.G., 2017. Multi-fault earthquakes with kinematic and
471   geometric rupture complexity : how common ? INQUA Focus Group Earthquake Geology and
472   Seismic Hazards.

473 Raimondo, T., Collins, A.S., Hand, M., Walker-Hallam, A., Smithies, R.H., Evins, P.M., Howard,
474   H.M., 2010. The anatomy of a deep intracontinental orogen. Tectonics 29.
475   https://doi.org/10.1029/2009TC002504

476 Stewart, A.J., 1995. Western extension of the Woodroffe Thrust, Musgrave Block, central Australia.
477   AGSO J. Aust. Geol. Geophys. 16, 147–153.

478 Wade, B.P., Kelsey, D.E., Hand, M., Barovich, K.M., 2008. The Musgrave Province: Stitching north,
479   west and south Australia. Precambrian Res. 166, 370–386.
480   https://doi.org/10.1016/j.precamres.2007.05.007

481 Wesnousky, S.G., 2008. Displacement and geometrical characteristics of earthquake surface ruptures:
482   Issues and implications for seismic-hazard analysis and the process of earthquake rupture. Bull.
483   Seismol. Soc. Am. 98, 1609–1632. https://doi.org/10.1785/0120070111

484 Wex, S., Mancktelow, N.S., Camacho, A., Pennacchioni, G., 2019. Interplay between seismic fracture
485   and aseismic creep in the Woodroffe Thrust, central Australia – Inferences for the rheology of
486   relatively dry continental mid-crustal levels. Tectonophysics 758, 55–72.
487   https://doi.org/10.1016/j.tecto.2018.10.024

488

489 **Appendix A**

490 **Methods for digitising vertical displacement data and benchmark data**

491 Vertical offset measurements are presented in Tables 1 – 4 of Bowman and Barlow (1991) alongside
492 decimal and UTM coordinates. These tables were copied from PDF into excel and thoroughly

493 checked for copy errors. The CSV of decimal degrees and vertical displacements was then imported
494 into GIS and checked against the surface rupture trace. A short script[2] was used in QGIS attribute
495 manager field calculator to extract the distance of each vertical offset measurement along the surface
496 rupture trace. The shape file was extracted into a final CSV with x-y coordinates, vertical offset
497 measurements, and distance along fault data.

498 Three dip measurements are shown in sketches on survey plates of Bowman and Barlow (1991).
499 These were digitised based on the location of the closest survey point as previously imported from the
500 vertical offset tables. Two dip measurements from trenches described in Machette et al. (1993) were
501 digitised directly from trench sites identifiable on high resolution satellite imagery, cross-referenced
502 to the trench location shown on Plate 2 of Machette et al. (1993).

---

[2] line_locate_point(geometry:=geometry(get_feature('Line', 'id', '1')), point:=$geometry)